Cement & Concrete Composites 42 (2013) 20–29

Contents lists available at SciVerse ScienceDirect

Cement & Concrete Composites

journal homepage: www.elsevier.com/locate/cemconcomp

Simple methods to estimate the influence of limestone fillers on reaction and property evolution in cementitious materials

Aditya Kumar [a], Tandre Oey [a], Seohyun Kim [a,1], Davis Thomas [a], Sondos Badran [a,1], Jialin Li [a], Fabio Fernandes [a], Narayanan Neithalath [b], Gaurav Sant [a,c,*]

[a] Laboratory for the Chemistry of Construction Materials (LC2), Department of Civil and Environmental Engineering, University of California, Los Angeles, CA, USA
[b] School of Sustainable Engineering and the Built Environment, Arizona State University, Tempe, AZ, USA
[c] California Nanosystems Institute, University of California, Los Angeles, CA, USA

ARTICLE INFO

Article history:
Received 17 November 2012
Received in revised form 3 May 2013
Accepted 8 May 2013
Available online 20 May 2013

Keywords:
Setting
Cement
Limestone
Hydration
Strength

ABSTRACT

A commercial interest in sustainable cementing materials is driving efforts to reduce the use of cement in concrete. Limestone fillers are a promising direction towards achieving such cement use reductions. In spite of increasing filler use, little information is available to rapidly estimate the influences of limestone fillers, and more importantly filler fineness on reaction and property development. This work develops simple models to predict the effect of particle size classified limestone on hydration reactions and compressive strength development. The method builds on a relativistic basis, such that enhancements and alterations in reactions and properties are described in relation to a given control (pure cement) mixture. The prediction method considers aspects such as: (1) accelerations in reactions, (2) changes in inter-particle spacing as linked to the limestone filler's fineness and (3) a porosity increase with increasing cement replacement. The predictive power of the approach is demonstrated for a variety of mixtures composed using three ASTM C150 compliant cements and forwards a basis for developing mixture proportioning strategies, such that *apriori* estimations of the mixture response (reaction rate and mechanical properties) can be used to optimize binder proportioning and thus strategize new methods to limit cement use in concrete construction applications.

1. Introduction and background

CO_2 emissions resulting from cement production are a cause of considerable concern to the concrete construction community [1]. To limit the CO_2 impact of cement production and use, the construction industry is making ever more substantial efforts to reduce and optimize the use of cement in concrete. Substantial amongst these efforts are initiatives to utilize high volumes of mineral substances (e.g., fly ash, limestone, quartz, etc.) to replace portland cement in concrete [2–8]. While much desired from a sustainability basis, large reductions in the portland cement content can be detrimental due to their role in delaying and/or depressing property development (e.g., setting, strength gain), and hence the constructability of low cement content binders [9]. Such reductions in constructability are a substantial obstacle to the commercial use and deployment of low-cement content binder systems.

In spite of substantial advances, concrete mixture proportioning is yet an empirical, parametric process in which a large number and combinations of materials require evaluation before an optimum mixture proportion is achieved. Clearly, as any parametric process, this approach is laborious and time-consuming. Thus, to ease the proportioning of sustainable mixtures, it would be beneficial if a cement or concrete producer may be able to virtually estimate the response of a mixture's mixture's binder fraction in relation to hydration and property development – as the cement content is systematically reduced.

Towards satisfying both of these needs, i.e., developing sustainable cementing materials and improving strategies for their proportioning, this research advances simple relationships based on chemical and physical indicators which can be used to predict the influence of size classified limestone additions on hydration and strength development in these materials. Based on a large experimental dataset, the approach is developed and applied for three ASTM C150 compliant cements, for cement replacement levels ranging between 0–50% (by mass) by limestone filler. Special attention is paid to limestone as its ability to serve as a "*mineral*

* Corresponding author at: Laboratory for the Chemistry of Construction Materials, Department of Civil & Environmental Engineering, University of California, Los Angeles, CA, USA. Tel.: +1 310 206 3084.
E-mail addresses: adityaku@ucla.edu (A. Kumar), gsant@ucla.edu (G. Sant).

[1] At the time, High-School Summer Research Program '12 (HSSRP'12) participants at UCLA Engineering.

0958-9465/$ - see front matter © 2013 Elsevier Ltd. All rights reserved.
http://dx.doi.org/10.1016/j.cemconcomp.2013.05.002

Table 1
The phase compositions of the ordinary portland cements used in this study.

ID	Phase	Mass%	ID	Phase	Mass%	ID	Phase	Mass%
OPC I/II	C_3S	63.10	OPC II/V	C_3S	62.60	OPC III	C_3S	63.30
	C_2S	12.89		C_2S	11.76		C_2S	10.31
	C_3A	3.67		C_3A	4.58		C_3A	3.93
	C_4AF	10.83		C_4AF	13.92		C_4AF	14.22
	Na_2O Equivalent	0.38		Na_2O Equivalent	0.55		Na_2O Equivalent	0.47

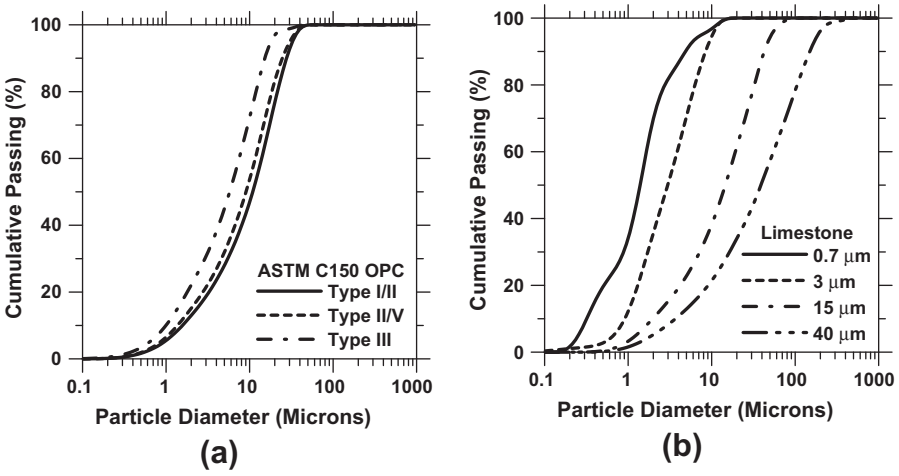

Fig. 1. Particle size distributions for the: (a) cement and (b) limestone used in this study.

acceleration agent" advances opportunities to reduce the cement content in a binder, by accelerating hydration product formation at early ages [10]. Thus the work advances: (1) simple strategies for concrete technologists to virtually estimate the influence of the cement replacement level and limestone fineness on reactions and property development and (2) enables a means to limit the need for time consuming, parametric mixture evaluations as are common today. The results have broad implications on refining mixture proportioning strategies, and introducing new approaches which can be used to proportion the next generation of binders with a reduced cement content.

2. Materials, mixing procedures and methods

Three ASTM C150 compliant cements were used in this study [11]. The phase compositions of the cements used are provided in Table 1. The limestone powders used are, nominally pure, commercially available, particle size classified products produced by OMYA A.G[2]. The particle size distributions (PSD, Fig. 1) of all the solids were measured using light scattering using isopropanol and sonication for dispersing the powders to primary particles. The uncertainty in the scattering measurements was determined to be 6% based on measurements performed on six replicates assuming the density of cement and limestone to be 3150 kg/m^3 and 2700 kg/m^3 respectively. Cementitious paste mixtures were prepared using de-ionized (DI) water at a fixed water-to-solids ratio (w/s = 0.45) as described in ASTM C305 [11]. To better understand the role of the limestone filler, the cement content was progressively reduced, by replacement in 10% increments, from 0–50% (mass-basis) by limestone powders of varying median particle (d_{50}, Table 2) sizes. Other mixtures were prepared with w/c equivalent to those obtained for the cement replaced systems, ranging from w/c = 0.45-to-0.643.

The influence of powder additions (cement replacement) on the solid surface area of the system is described using an area multiplier (AM, unitless) as shown in Eq. (1):

$$\mathrm{AM} = \frac{100 + \frac{(r.\mathrm{SSA_F}) + ((100-r).\mathrm{SSA_c})}{((100-r).\mathrm{SSA_c}}}{100} \quad (1)$$

where: r (mass%) is the percentage replacement of cement by limestone filler and $\mathrm{SSA_C}$ and $\mathrm{SSA_F}$ (m^2/g) are the specific surface areas of the cement and limestone respectively - – calculated using the particle size distribution of the powder materials, while assuming spherical particles. Thus, the AM is a scaling factor that describes the change in solid surface area induced by filler addition in comparison to the surface area provided by a unit mass (1 g) of cement (reactant). In other words, AM is the surface area of filler per unit surface area of cement in the system. The greater this quantity is, either because the filler is finer or because it is present in greater amounts, the more AM will exceed unity. It should be noted that the calculation of the AM is subject to uncertainties that stem from measurements of the particle size distributions and the assumption of spherical particle shape.

Table 2
Nominal d_{50} and specific surface area (SSA) values for the cement and limestone powders, calculated using their measured particle size distributions shown in Fig. 1.

	ASTM C150 OPC		Size classified limestone		
Powder ID	d_{50} (μm)	SSA (m^2/kg)	Powder ID (μm)	d_{50} (μm)	SSA (m^2/kg)
Type I/II	9.83	486.00	0.7	1.40	2592.10
Type II/V	8.94	538.02	3	2.98	1353.20
Type III	5.61	780.27	15	14.87	399.20
			40	40.10	228.60

[2] Certain commercial materials and equipment are identified to adequately specify experimental procedures. In no case does such identification imply recommendation or endorsement by the University of California, Los Angeles or Arizona State University, nor does it imply that the items identified are necessarily the best available for the purpose.

Table 3
Constants used in calculation of the calorimetric parameters using Equation (2).

Parameters	Slope (mW/g_{cement}.h)	Heat flow at peak (mW/g_{cement})	Inverse time to peak (h)
C1	−1.0013	2.4800	0.0949
C2	1.8359	5.5871	0.2359
C3	0.9189	0.8715	0.3311
C4	0.8600	1.4567	1.5222
A	0.0040	0.0020	0.0010
B	−1.1000	-0.1037	0.5672

The influence of cement replacement on the rate of reactions was tracked using isothermal conduction calorimetry. A Tam Air isothermal calorimeter (TA Instruments, DE, USA) was used to determine the heat evolved during hydration at a constant temperature condition (25 °C). The thermal power and energy were used to assess the influence of powder additions on reaction kinetics and the cumulative heat release of the cementitious mixtures.

The compressive strength of cubic (50 mm x × 50 mm x × 50 mm) specimens cured at 25 ± 0.2 °C, in a sealed condition was measured as described in ASTM C109 at 1, 3, 7 and 28 days [11]. The compressive strength value reported is typically the average of three specimens. The coefficient of variation (CoV) in the measured compressive strength was determined to be around 10% for samples cast from the same mixing batch.

The time of initial and final set of the paste mixtures was determined as described in ASTM C191 at 25 ± 3 °C [11]. In the ASTM C191 standard, the single laboratory precisions are listed as 12 min (0.2 h) and 20 min (0.33 h) for the time of initial/final set respectively.

3. Experimental results and discussion

Fig. 2 shows the influence of: (a) cement type, (b) limestone particle size (fineness) and (c) the cement replacement level on the rate of hydration reactions. It is noted that, in general, an increase in the cement fineness, filler fineness, or filler content acts to increase the rate of chemical reactions. This increase (i.e., acceleration) manifests as a left-shift of the rate curve and elevation in the heat flow at the main peak [12,13]. While this effect is somewhat influenced by the chemistry of the system and the nature of the filler agent this response is as expected, as an increase in the fineness of the cement or the limestone, in general, increases

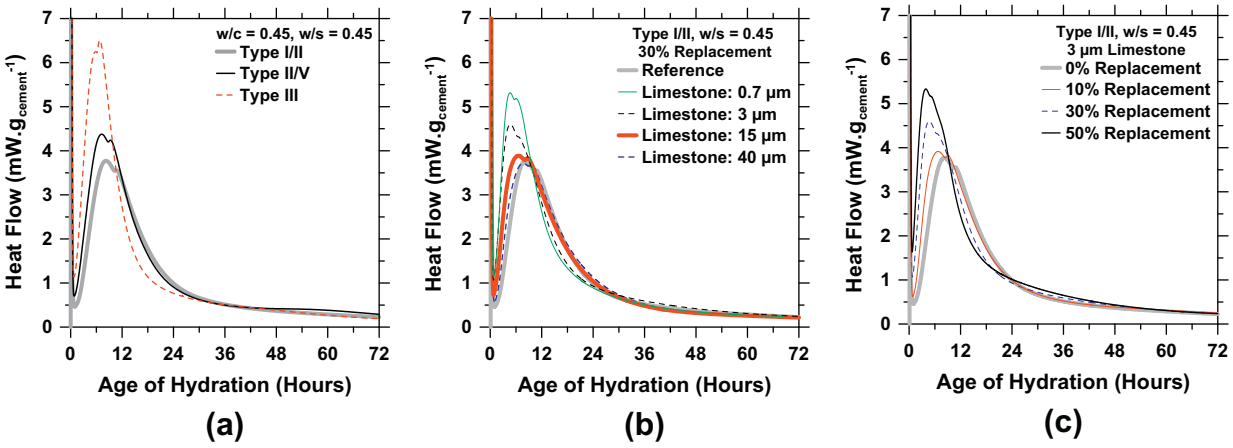

Fig. 2. Representative graphs showing the rate of heat release measured using isothermal calorimetry to highlight the influence of: (a) cement type, (b) limestone particle size and (c) cement replacement level on hydration reaction rates.

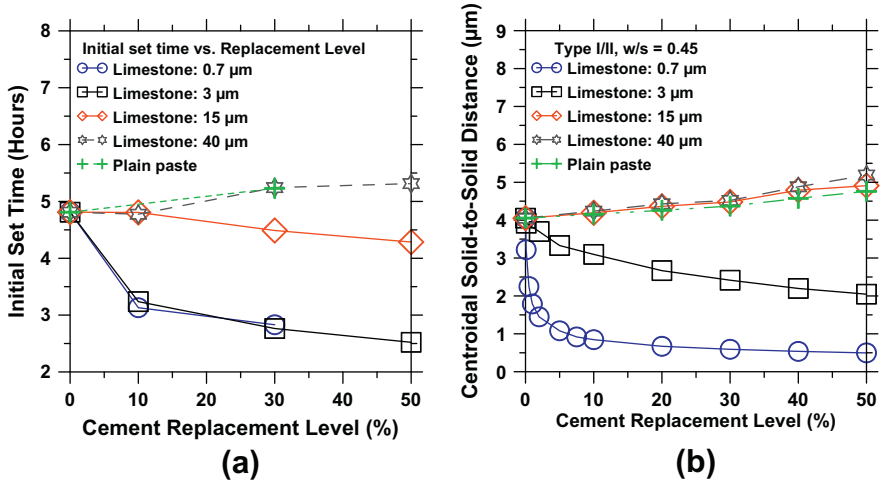

Fig. 3. Representative graphs showing: (a) the experimental time of initial set and (b) the calculated centroidal solid-to-solid distance functions for varying cement replacement levels. It should be noted that a plain paste for a cement replacement level of 30% has a w/c equivalent to a paste containing 30% limestone; i.e., $w/c = w/s = 0.643$ in the first case, while $w/c = 0.643$ and $w/s = 0.45$ in the latter case.

the surface area available for reactions resulting in an acceleration [13].

Fig. 3(a) shows the influence of the cement replacement level and limestone particle size on the time of initial set of paste mixtures. As noted by Bentz et al., fine limestone additions are an efficient means for decreasing the time of initial set of cementitious mixtures [9]. This reduction of initial set time is a function of two effects including: (1) an acceleration in hydration reactions induced by limestone additions (as shown in Fig. 2) and (2) reductions in interparticle spacing produced (at a constant liquid content) by the addition of limestone, so long as the limestone is finer than the cement that it replaces.

To study the particle spacing effect in detail, a microstructural stochastic packing algorithm with periodic boundary conditions was implemented [14,15]. This algorithm, which uses the measured particle size distribution and volumetric fractions of materials as inputs (cement, limestone, and water), packs spherical particles in a 3D-REV (representative element volume) of 500 x $\times$ 500 x $\times$ 500 μm^3. Microstructural generation and packing is permitted such that the minimum centroidal distance (C_D, μm, for size distributed particles) between two proximal particles is always greater than the sum of their radii ($C_D > r_1 + r_2$). The packing algorithm packs the REV while iteratively analyzing and placing particles at random locations within the microstructure in relevance to two packing criteria: (1) the size (largest to smallest), and number of particles (information which is determined by the particle size distribution), within the constraint that particles cannot contact and (2) the input volume fractions of the phases are satisfied, as described by the *w*/*s* of a given mixture (see Fig. 4). Once the sought packing is achieved, the mean solid-to-solid centroidal distance in the REV is calculated as follows: (a) 100 particles are randomly selected in the microstructure, (b) for each particle p_i, the solid-to-solid centroidal distance is computed with respect to all neighboring particles located within a distance of 5 μm away from the surface of p_i to identify its closest neighboring particles and (c) the mean solid-to-solid centroidal distance is calculated by averaging the centroidal distances calculated for all 100 particles. It should be noted that the selection of 100 random particles was made, as beyond this point the calculated centroidal distances between particles were noted to change very slightly, even if the number of analyzed solid particles was increased substantially. The mean solid-to-solid centroidal distance calculated as a function of the cement replacement level is shown in Fig. 3(b) [16,17].

An examination of Figs. 3 and 4 provides qualitative insights into the influence of mineral filler fineness and the cement replacement level on the trends observed in the time of initial set. Initial set is chosen as a time of relevance as this is an interval at which the solids are expected to be bridged (i.e., percolated) in 3D from contacts resulting from cement hydration [20] – a point to be differentiated from simple surface to surface contacts between particles [18]. It is noted that fine fillers (i.e., with a high specific surface area), decrease the time needed to achieve initial set at a given cement replacement level. This trend is observed to systematically invert as either the filler size or the water content (*w*/*s*) of the mixture is increased; e.g., a paste with *w*/*c* = 0.643 and a paste with *w*/*s* = 0.45 (*w*/*c* = 0.643), with 30% limestone replacement by 40 μm limestone both show a similar time of initial set (see Fig. 3a). This result suggests that the time of initial set is strongly correlated with the initial dispersion of the solid particles. Since fine fillers reduce, and coarse fillers increase, the interparticle spacing (Fig. 3b; a consequence of better packing) [19], this observation indicates that a decrease in the inter-particle spacing increases the propensity for 3D solid-percolation, by reducing the time/extent of hydration required to achieve set [20,41] – an effect which is only *magnified* by the mineral acceleration induced by limestone [13]. While consistent, these results can be treated as *qualitative only*, as the packing algorithm used does not consider the effects of (enhanced) agglomeration that may manifest in *"un-plasticized"* systems when fine fillers are used to replace portland cement. As a result, the actual distances between solid particles may be much smaller (or larger) than those depicted in Fig. 3(b), preventing *apriori* quantifications and predictions of the time of initial and final set [21,22].

Fig. 5 shows the evolution of compressive strength for mixture parameters including: (a) the limestone particle size, (b) the cement replacement level and (c and d) the effects of *w*/*c*, for mixtures with/without cement replacement by limestone. From Fig. 5(a), it is noted that, at low replacement levels, the early age (1 day) strength is a function of the limestone particle size, with the highest strength (though slightly so) being produced by the 0.7 μm limestone filler [23], at 10% cement replacement. This observation is unsurprising, as the acceleratory and packing effects of limestone, which improve with decreasing particle size, are expected to result in such a trend. This effect diminishes with increasing particle size, with the measured compressive strength decreasing accordingly. From Fig. 5(b), it is noted that the strength decreases with increasing cement replacement. This effect starts to attain increasing relevance, broadly, for cement replacement levels in excess of 10% (mass basis). Finally, Fig. 5(c) shows the influence of *w*/*c* equivalence for mixtures with and without cement replacement. Here, it is noted that mixtures which contain limestone show higher strengths up to 7 days, but the strengths measured at 28 days are much more similar to the equivalent plain paste systems.

The *w*/*c*-strength response noted in Fig. 5(c) can be explained by considering the evolution of the capillary porosity (i.e., as defined by Powers and coworkers [31]) in these mixtures which is shown in Fig. 5(d). As such, it can be rationalized that the higher strength of the limestone containing pastes is an outcome of their lower

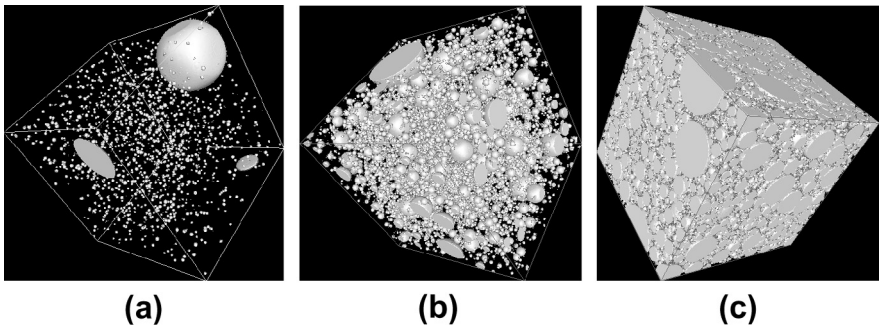

Fig. 4. Generation of virtual microstructures with varying space-to-solids (i.e., water-to-solids ratios) which show the influences of solid particle sizes and individual phase fractions on the distances between particles. The 3D images shown correspond to the generation of representative elementary volumes (REVs) for *w*/*s* (mass basis) of: (a) 5.0 (b) 0.5 and (c) 0.1.

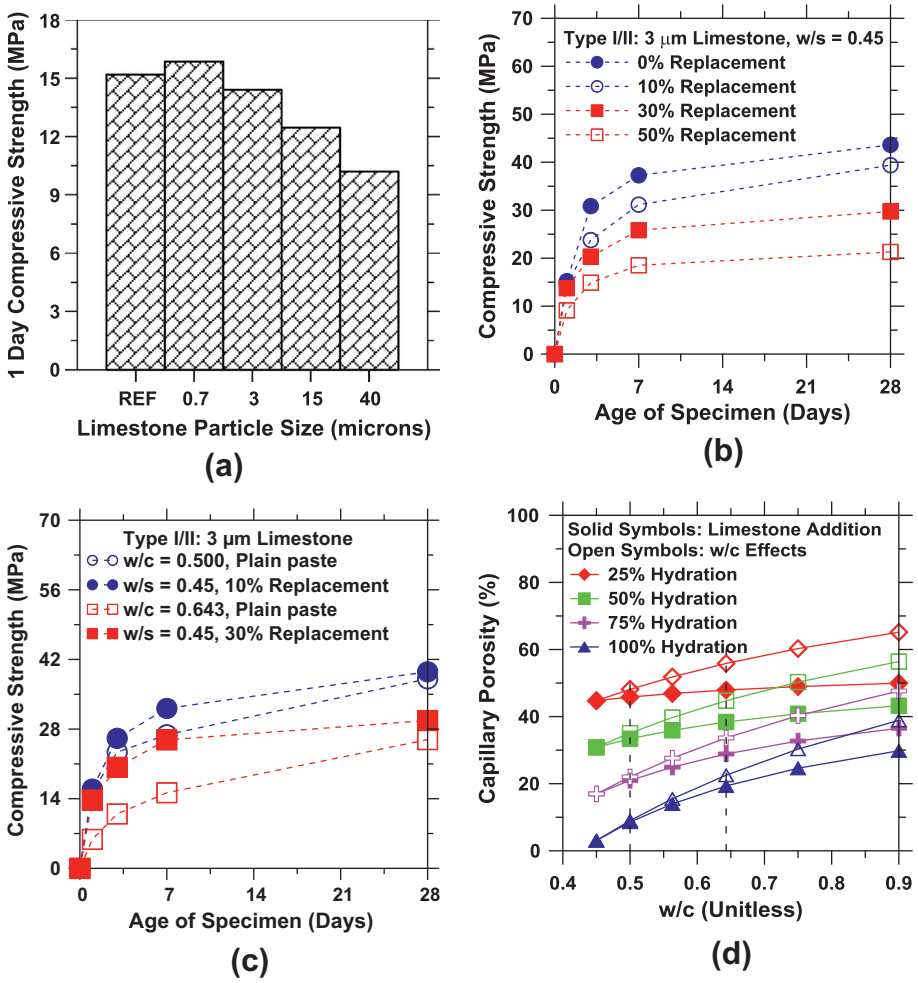

Fig. 5. Representative graphs showing strength evolution as a function of time: (a) for varying limestone particle sizes, (b) for varying cement replacement levels, (c) to compare the effects of *w*/*c* equivalence and cement replacement on the measured compressive strength and (d) shows the capillary porosity at different extents of hydration as a function of *w*/*c* and limestone addition (at the same *w*/*c*) as calculated using Powers Model [31]. The dashed vertical lines show *w*/*c* equivalence points corresponding to 10% (*w*/*c* = 0.50) and 30% (*w*/*c* = 0.643) replacement (mass basis) of cement by limestone for mixtures composed at *w*/*s* = 0.45.

capillary porosity – as caused by a higher solid loading. Fig. 5(d) also explains why mixtures composed at an equivalent *w*/*c*, both with and without limestone[3], show increasingly similar strengths with increasing age and thus increasing hydration. With increasing hydration, for the *w*/*c* evaluated, the ever diminishing difference in the capillary porosity (Fig. 5d) ensures that materials, with and without limestone, composed at similar *w*/*c* will within limits, exhibit similar strengths. This observation (i.e., similar strength after 28 days) may also be partially ascribable to the fact that limestone is a much softer inclusion than either the unhydrated clinker phases, or the hydration products formed and hence may be the *weak-link* in the system at later ages [24–26].

To describe the effects of a reduction in the cement content on reactions, a set of plain cement pastes were prepared with *w*/*c* ratios corresponding to the actual cement content in the systems with partial filler replacement levels ranging from 0%-to-30% (mass basis, see Fig. 6a). It is noted that the calorimetry curves overlap, indicating equivalent reaction kinetics (rate/extent) –– suggesting that these systems hydrate equivalently over the course of the experiment (i.e., over the first seven 7 days). Results of this nature, which have been observed previously, are expected for pastes which hydrate (within limits) in a *water-sufficient* system [13,27,28]. However, in spite of equivalence in hydration, it is noted that the compressive strength of pastes decreases with an increase in their *w*/*c* (Fig. 6b). This result is in accordance with trends in the calculated gel-space ratio, where the gel-space ratio and the strength increase with decreasing *w*/*c* [29–31].

Recently, Bentz and co-workers showed unambiguously that heat evolution through hydration is a strong and direct measure of mechanical property (i.e., compressive strength) development in cementitious materials [32,33]. To establish such correlations between the extent of hydration and the evolution of properties, the compressive strength values for all paste systems were cast as a function of the cumulative heat released normalized by the water content of the mixture at an age of 1, 3, 7 and 28 days as shown in Fig. 7. Here, it should be noted that the measured heat is normalized by a mixture's water content (mass or volume basis, assuming the density of water, $\rho_W = 1$ g/cm^3), as the initial water content is a measure of the initial porosity of the system, i.e., space that can be progressively filled by the reaction products to achieve better properties. As seen in Fig. 7, the heat-strength data-cloud is strongly correlated with a majority of data points lying within $a \pm 20\%$ bound of the linear best fit line. It should be noted that the best fit line shows a non-zero *x*-intercept ($Q_0 \sim 214$ J/cm^3), indicating that a critical amount of hydration needs to occur after

[3] These explanations consider limestone to behave as an *essentially inert* filler in the system. However, it should be noted that this explanation would be subject to change, if for example, the formation of a substantial quantity of carboaluminate phases were expected in a given reactant system/s.

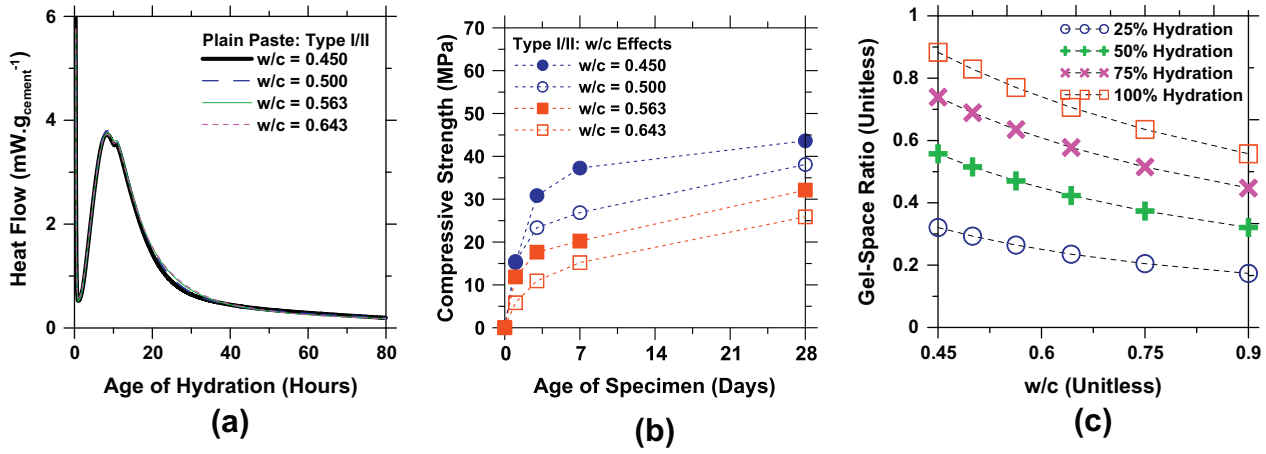

Fig. 6. The role of *w/c* on the: (a) hydration response and (b) strength evolution and (c) the evolution of the gel-space ratio in the system.

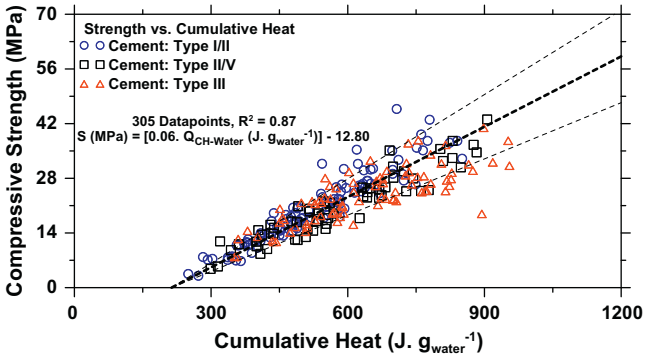

Fig. 7. The compressive strength as a function of cumulative heat release, normalized by the initial water content for all the mixtures evaluated in this study. The thick dashed line represents the (linear) best fit line with 20% bounds placed on either direction (thin lines).

which the material starts to gain (measurable) strength. However, it is also noted that once strength development begins ($Q_0 > 214$ J/cm^3), the rate of strength gain is very similar for all the paste mixtures. Overall the linear correlation demonstrated is consistent with recently published studies [32,33] and, provides a *predictive* basis to link the progress of reactions to mechanical properties as described in further detail below.

4. Development of a prediction method for the progress of hydration reactions

To build relationships to describe the influence of limestone fineness on the hydration response of each cement, unique calorimetric parameters including the: (a) slope during the acceleration period, (b) heat flow at the main peak and (c) inverse of time needed to achieve the heat peak are plotted as a function of the AM (Fig. 8). These relationships are then fitted using separate 4-parameter sigmoid growth functions as shown in Eq. (2) and Table 3:

$$\mathrm{CP(AM)} = M_F\left|C_2 + \left|\frac{(C_1 - C_2)}{\exp\left(\frac{\mathrm{AM}-C_4}{C_3}\right)}\right|\right| \tag{2a}$$

$$\text{where } M_{F,CP} = A.\mathrm{SSA_C} + B \tag{2b}$$

where: CP is a given calorimetric (i.e., effect) parameter, C_1, C_2, C_3 and C_4 are generic fitting constants for each calorimetric parameter, the values of which are listed in Table 3, and AM is the area multiplier (unitless; cause parameter). $M_{F,CP}$ is a multiplication factor (unitless, Fig. 8d) which scales the fitting function (Eq. (2b)) in relation to the surface area of the cement (m^2/kg) and includes A and B as fitting constants pertinent to a given calorimetric parameter (i.e., slope during the acceleration period, heat flow at the main peak or inverse of time needed to achieve the heat peak).

Importantly, the form of Eq. (2) is generic enough to be able to describe each calorimetric parameter over a wide range of limestone particle sizes and cement replacement levels (AMs). This suggests that, once quantified for a single cement across a range of replacement levels or more correctly AMs, the calorimetric parameters for any other cement/limestone combination can be sketched, with apriori knowledge of the cement fineness (Fig. 8d) and the reaction response of a plain cement paste (see below). Of course, it should be noted that this approach is limited to cements which show *broadly similar* chemistries (i.e., major phase compositions).

The approach used to predict the hydration response applies a family of piecewise linear functions to describe the heat flow response, through the different stages of hydration including: dissolution, induction, acceleration, deceleration, steady state, etc. This approach is relativistic in that it uses the: (1) reaction rate curve applicable to the reference plain cement paste for a given cement and (2) calorimetric parameters described using Eq. (2) and shown in Fig. 8 to predict the rate of reactions when the cement content is reduced – by replacement with particle size classified limestone. Based on these aspects, while the pre-acceleration regime features are assumed to be similar independent of the cement replacement level, post-induction regime features are described as a function of the AM; i.e., fineness and quantity of the cement and limestone in a given mixture. These piecewise linear functions for prediction of heat up to 3 days of hydration are described by Eq. (3).

$$P_{HF}(t) = M_{HF}(t) \text{ for } (t < t_{IND,Ref}) \tag{3a}$$

$$P_{HF}(t) = [\mathrm{Slope_{ACC}}.t] \text{ for } (t_{IND,Ref<t<t_{PEAK}}) \tag{3b}$$

$$P_{HF}(t_{PEAK}) = [\mathrm{Max}((\mathrm{Slope_{ACC}}.t_{PEAK}), (H_{PEAK}))] \text{ for } (t_{PEAK} < t < t_{PEAK} + 3\text{ h}) \tag{3c}$$

$$P_{HF}(t) = [P_{HF}(t) - 0.35.\mathrm{Slope_{ACC}}.(t - (t_{PEAK} + 3))] \text{ for } (t_{PEAK} + 3\text{ h} < t \text{ and } P_{HF}(t) > 1.00) \tag{3d}$$

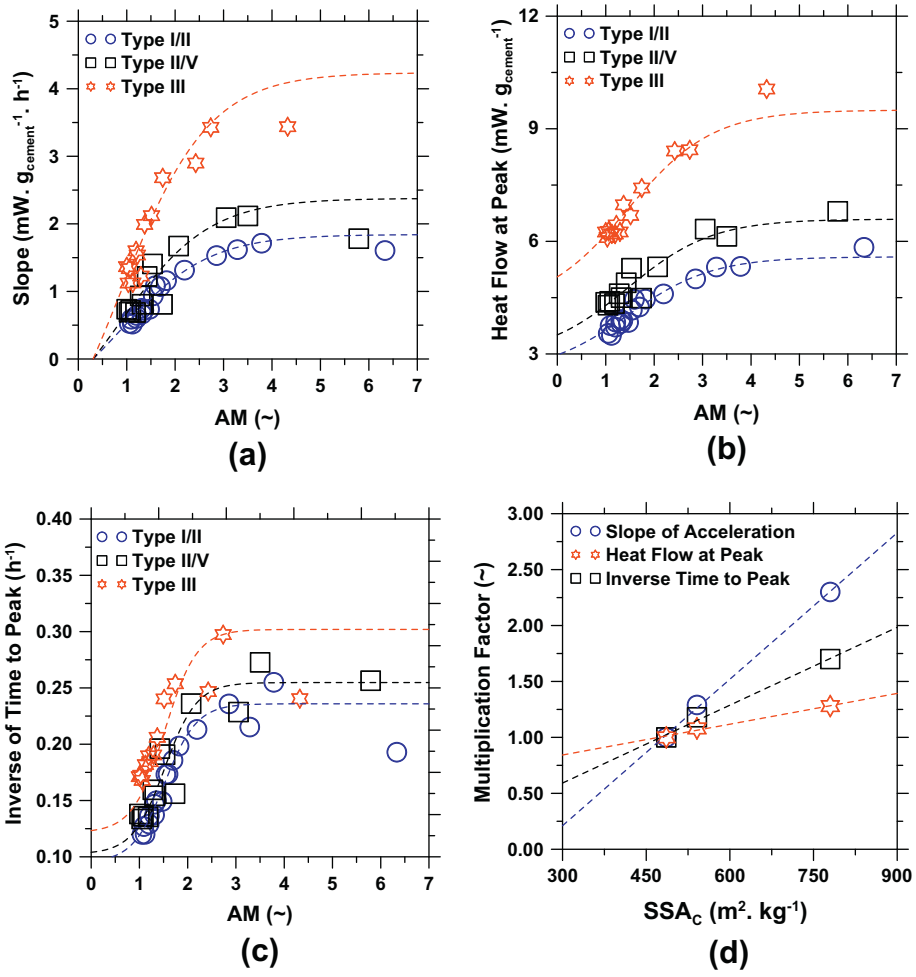

Fig. 8. Calorimetric parameters for cementitious (paste) mixtures as a function of AM for: (a) slope in the acceleration period, (b) heat flow at peak, (c) the inverse of time to peak and (d) the multiplication factors for each calorimetric parameter as a function of the cement fineness. The dashed lines represent the best mathematical fit to the experimental datasets.

$$P_{HF}(t) = [1.289 - 0.017.(t)] \; for \; (t \leq 72 \text{ h} \; and \; 0.00 \leq P_{HF}(t) \leq 1.00) \tag{3e}$$

$$P_{CH}(t) = \int_0^t P_{HF}(t)dt \; for \; (0 \leq t \leq 72 \text{ h}) \tag{3f}$$

where: $P_{HF}(t)$ is the predicted heat flow at a given instant in time (mW/g$_{CEM}$), $M_{HF}(t)$ is the heat flow measured using isothermal calorimetry (mW/g$_{CEM}$) for a plain cement paste system for a given cement, t is the reaction time (ranging between 0– and 72 h), $t_{IND,Ref}$ is the reaction time at which the induction period terminates for the plain cement paste system determined by reverse projection (to the

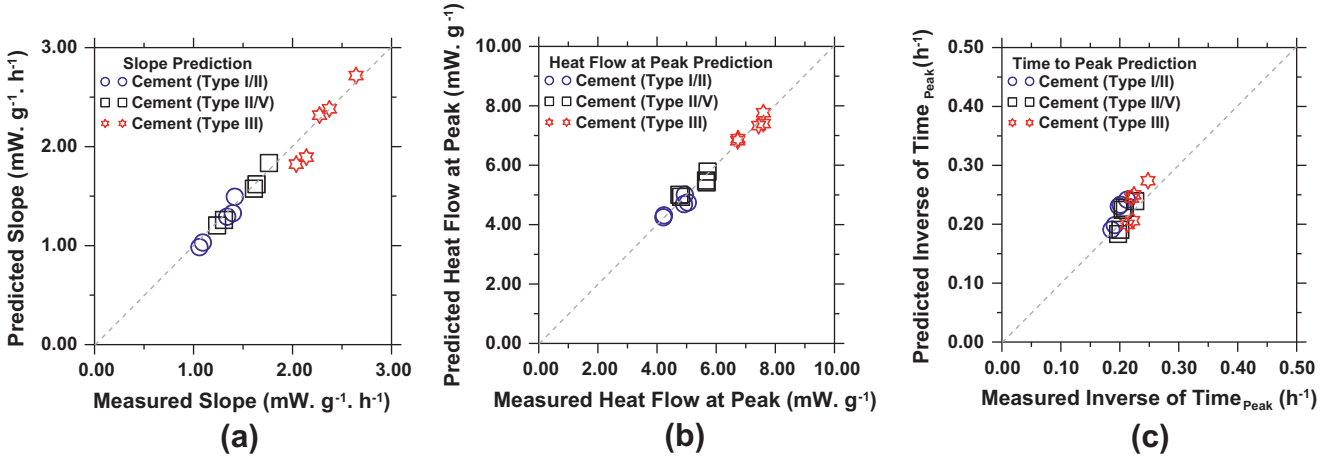

Fig. 9. A comparison of measured and predicted parameters for mixed limestone systems for mixtures composed at a given cement replacement level for: (a) slope during the acceleration period, (b) heat flow at peak and (c) inverse of time to the main heat peak.

x-axis) of the heat flow response during the acceleration regime (hours), t_{PEAK} (hours) and H_{PEAK} (mW/g_{CEM}) are the reaction time and magnitude/amplitude corresponding to the main heat peak, $Slope_{ACC}$ is the slope of the heat flow curve during the acceleration regime (mW/g_{CEM}/hour) and $P_{CH}(t)$ is the predicted cumulative heat released due to chemical reactions in a given reaction time period (J/g_{CEM}). Per the equations above, the following assumptions are made: (a) the addition of limestone does not substantially alter the pre-acceleration features of hydration, (b) the reaction maintains its maximum rate for 3 h independent of the level of cement replacement and (c) the reaction decelerates at a fixed rate until a heat flow value of 0.00 mW/g_{CEM} is achieved.

$$P_{CH}(7\ \text{days}) = [1.20P_{CH}(72\ \text{h})] \tag{4a}$$

$$P_{CH}(28\ \text{days}) = [1.32P_{CH}(72\ \text{h})] \tag{4b}$$

Given the relatively "linear" evolution of heat after early times (i.e., after 72 h) for typical mixtures, the heat evolved at 7 and 28 days can be estimated with a very high level of accuracy by simply multiplying the 3 day heat value by a constant factor as shown in Eq. (4). While this approach is simplistic, for the range of mixtures considered herein, this simple multiplication yielded 7 and 28 day heat values with an accuracy greater than 95% suggesting that as a first approximation its application may be broader than expected. While the relations shown below are empirical, in certain cases, estimations of this nature may be essential, e.g., to determine the extent of heat released after 28 days of hydration, which may be a non-trivial task with some isothermal calorimetry instruments (due to signal-to-noise, or heat sensitivity limitations), without having to resort to heat of solution determinations [33].

The validity and robustness of the prediction method is tested using a variety of *mixed systems* which remain undefined in the training set as shown in Fig. 10. Here, for a given cement type, and a single cement replacement level, by limestone (30%, mass basis), two gradations (i.e., powders of differing median particle sizes) of limestone are intermixed in equal parts (e.g., 50%–50% by mass blend of the 0.7 and 3 μm) rather than a single gradation (e.g., 0.7 μm) prior to being used to replace cement in the mixture [34]. In spite of its very simple basis, it is noted that that a piecewise linear approach, is able to very accurately predict the calorimetric parameters and the heat flow and cumulative heat release curves for the mixed systems (as also the other systems defined in the training set, *not shown*) to describe the evolution of hydration reactions in these materials – as shown in Figs. 9 and 10.

While the method applies very well for the systems evaluated in this study, substantial changes in the cement chemistry and/or the use of fillers (compositionally) different from limestone may necessitate modifications in the formulas used. It is also important to note that, while increasing area (i.e., cement and/or limestone fineness) does accelerate reactions, broadly for AM $\geqslant$ 4, any further increase in surface area (i.e., filler fineness) has limited benefits. This is likely related to: (1) enhanced agglomeration of very fine filler particles, which would reduce their exposed surface area and trap water in flocs inducing a less than expected acceleration in hydration rates and/or (2) a surface area saturation effect, wherein the available surface area is far more than needed for reaction of the available quantity of cement, resulting in the observed plateau of the measured reaction parameters [13]. However, the approach is useful in that, for a reasonably broad selection of cement types and limestone fineness, it is able to describe the evolution of hydration reactions in cementing systems in relation to the cement and filler fineness. Simplistic models of this nature are useful in that they could be used to predict the acceleratory effects of limestone addition on binder hydration reactions – valuable information which could be used to proportion and *dial in* limestone

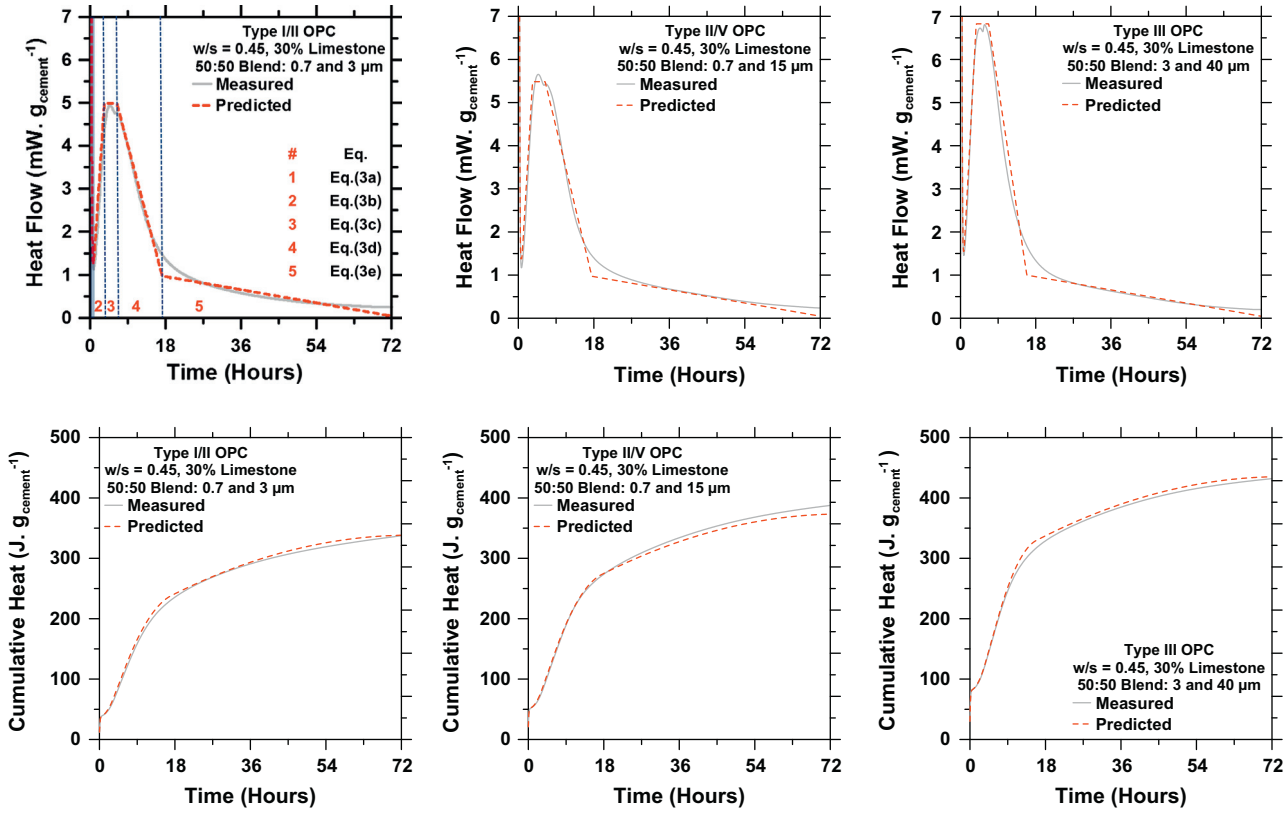

Fig. 10. Representative reaction curves which compare measured and calculated heat signatures for a variety of cement types and limestone sizes for: (top) heat flow and (bottom) cumulative heat release over the first 72 h: (a) shows the step specific use of different equations to sketch different regimes of the heat flow curve.

additions to address aspects of set and strength retardation in low-cement content and cement – replaced formulations.

5. Estimating mechanical property evolution from the heat release response

Fig. 7 demonstrated a strongly correlated relationship between the evolution of strength and heat release in a hydrating paste system. Significantly, it is noted that for a variety of cements with differing w/c, limestone replacement levels, and limestone particle size distributions, a single linear function is able to reliably link heat release through hydration (e.g., measured using calorimetry) to compressive strength development. In conjunction with the reaction prediction approach described above, a *virtual testing* approach e.g., see [35] can be forwarded to describe the influence of size classified limestone additions, cement fineness, and limestone replacement level on strength development. This approach which uses as inputs physical properties (i.e., SSA_C and SSA_F) and mixture proportions (i.e., w/s, r) of the materials, estimates strength development using Eq. (3) and a single calorimetry measurement of a reference (plain) cement paste [32,33,36,37]. Upon estimation of the cumulative heat release at a sought age, Eq. (5) can be used to estimate strength development in a cementitious paste mixture as:

$$S_{\text{Predicted}}(t) = 0.06P_{\text{CH-water}}(t) - 12.80 \quad (5)$$

where: $S_{\text{Predicted}}(t)$ is the predicted compressive strength at a given age (MPa), $P_{\text{CH-water}}(t)$ is the predicted cumulative heat flow at a given specimen age (e.g., 1, 3, 7 or 28 days) normalized by the initial water content of the mixture (J/g_{WATER}). It should be noted that this relationship is built on the basis of the linear-fit which best describes the data-cloud shown in Fig. 7.

The accuracy and robustness of the *strength prediction method* was validated for: (1) the mixed systems described above, constituted using two distinct gradations of limestone and (2) w/s = 0.45 mixtures in which 15% of the OPC (mass basis) is replaced by limestone powders having a median diameter of 0.7 and 3 μm. A replacement level of 15% (mass basis) achieved by post-blending is specifically chosen, in light of recent regulatory actions in the U.S., which allow OPC replacement (by limestone) at these levels. Procedurally, the predictions are accomplished as follows: first, the cumulative heat release of any given mixture through hydration is calculated at 1, 3, 7 and 28 days using Eqs. uations (3) and (4) and compared against experiment (Fig. 11a). It is noted that across a range of cement types, limestone gradations and OPC replacement levels, highly accurate heat predictions (average error ~ 2%) are obtained – see Figs. 9–11a. Second, the predicted cumulative heat values ($P_{\text{CH-water}}$) are input into Eq. (5) to predict the evolution of strength (Fig. 11b). Once again, the evolution of compressive strength for a broad range of mixtures can be predicted with an average error around 12% across all mixtures. In light of errors which accumulate across the: (1) heat release prediction (Fig. 11a) as also (2) the intrinsic variability encountered in compressive strength measurements of cement paste mixtures, this level of accuracy in strength predictions in a virtual test is surely acceptable.

Of course, it should be noted while this work develops the proposed approach specifically for limestone-based additions, similar approaches could be (and have been) applied and extended to other mineral fillers that are essentially inert at early ages (e.g., Class F fly ash, quartz, etc.) [32,33]. However, since different cement replacement agents exhibit different levels of mineral acceleration and intrinsic chemical reactivity (e.g., as being pozzolanic, or hydraulic), it is to be expected that the proposed approach would likely require refinement. Failing modifications, the accuracy of the prediction at later ages could be increasingly less precise due to changes in the reaction mechanism or process, e.g., as related to pozzolanic reactions which progress slowly. Additional complications would be introduced due to other factors including: (1) curing, i.e., saturated, sealed or mixed, as curing alters the nature and extent of strength development, more so in the case of water-deficient (low w/c) materials, (2) curing temperature, e.g., curing at ambient (25 °C) versus higher temperatures (60 °C) when microstructural changes can result in less than expected strength, inspite of equivalences in the extent of hydration (i.e., heat release) and (3) determinations of cement paste, mortar, or concrete specimens, due to the influences of aggregate volume fraction, gradation and aggregate stiffness [38–40] or substantial changes in the cement chemistry (e.g., blended cements). Pending verification, each of these complications requires further investigation to better understand, quantify and identify parameters needed to construct a more robust "*master curve*" to link heat release to strength development.

Inspite of the abovementioned limitations, it should be noted that practical restrictions on the application of this may be less relevant than suspected, as results from Bentz et al. [32,33] and ongoing studies at UCLA both suggest that while process and material parameters of the sort listed above do change the functional form of the *best-fit line* (see Fig. 7), the absolute error in compressive strength estimations is much more limited. Thus, in spite of its limitations, the approach is tremendously powerful in that it proposes a new means for concrete technologists to simplify and rationalize mixture proportioning protocols in use today, a critical step to advance the development of sustainable binders with a reduced cement content.

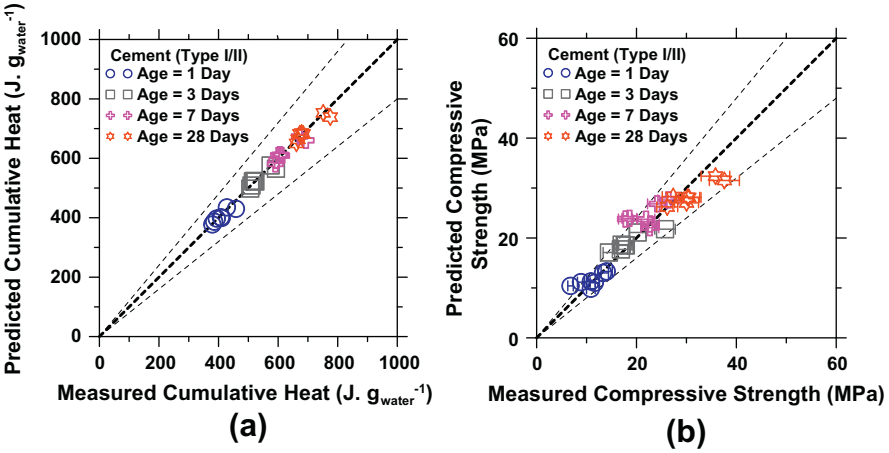

Fig. 11. A comparison of measured and predicted values for a variety of "blind tests" for: (a) cumulative heat release normalized by water content and (b) compressive strength evolution.

6. Summary and conclusions

This paper has described the influence of size classified limestone additions on reaction and property development in cementitious mixtures. The specific influences of limestone fineness, OPC type and replacement level are quantified by: (1) reaction rate parameters identified using isothermal calorimetry and (2) compressive strength evolution in paste mixtures. First, based on a large database of quantifications (i.e., a training set), a simple approach based on piecewise linear functions is developed to estimate the influence of size classified limestone additions on the rate and extent of reactions. Second, correlations between cumulative heat release through hydration and compressive strength development are tapped to identify a "*strength-heat master curve*" *(SHMC)*. In conjunction with the reaction prediction approach, the SHMC sets a basis for estimating the time dependent evolution of strength in paste mixtures composed using a variety of OPCs, for differing limestone gradations and OPC replacement levels. The robustness of the approach is verified using blind tests conducted against mixtures which remain undefined in the training set. The accuracy of these predictions is identified to be on the order of 2% and 12%, for cumulative heat and compressive strength estimations respectively, for timelines ranging from 1 day to 28 days. The approach builds a new basis to estimate heat and strength evolution in cementitious materials in the form of a modern evolution of the maturity method. Overall, the outcomes of the work have a significant impact on developing new methods to estimate, *apriori*, the influence of mixture proportions on hardened properties, and make innovative contributions towards advancing methods of binder formulation and proportioning that are in use today.

Acknowledgements

The authors acknowledge full financial support for this research provisioned by the University of California, Los Angeles (UCLA) and the National Science Foundation (CMMI: 1066583). The authors would also like to acknowledge the generous provision of materials by U.S. Concrete, Lehigh Cement and OMYA A.G. The contents of this paper reflect the views and opinions of the authors, who are responsible for the accuracy of the datasets presented herein. This research was conducted in the Laboratory for the Chemistry of Construction Materials (LC^2) and the Molecular Instrumentation Center (MIC) at the University of California, Los Angeles (UCLA). As such, the authors gratefully acknowledge the support that has made these laboratories and their operations possible. The last author would also like to acknowledge discretionary support for this research provided by the Rice Endowed Chair in Materials Science.

References

[1] Mehta PK. Global concrete industry sustainability. Concr Int 2009;31(2):45–8.
[2] Bentz DP. Powder additions to mitigate retardation in high volume fly ash mixtures. ACI Mater J 2010;107(5):508–14.
[3] Cost VT. Concrete sustainability versus constructability – closing the gap. In: presentation at international concrete sustainability conference. Boston; 2011.
[4] Kenai S, Soboyejo W, Soboyejo A. Some engineering properties of limestone concrete. Mater Manufact Proc 2004;19(5):949–61.
[5] Voglis N, Kakali G, Chaniotakis E, Tsivilis S. Portland-limestone cements: their properties and hydration compared to those of other composite cements. Cem Concr Compos 2005;27(2):191–6.
[6] Pera J, Husson S, Guilhot B. Influence of finely ground limestone on cement hydration. Cem Concr Compos 1999;21(2):99–105.
[7] Kadri EH, Aggoun S, De Schutter G, Ezziane K. Combined effect of chemical nature and fineness of mineral powders on portland cement hydration. Mater Struct 2009;43. 665-73.
[8] Kumar A, Oey T, Puerta Falla G, Henkensiefken R, Neithalath N, Sant G. A comparison of intergrinding and blending limestone on reaction and strength evolution in cementitious materials. Constr Build Mater 2013;43:428–35.
[9] Bentz DP, Sato T, De la Varga I, Weiss WJ. Fine limestone additions to regulate setting in high volume fly ash mixtures. Cem Concr Compos 2012;34(1):11–7.
[10] Gurney L, Bentz DP, Sato T, Weiss WJ. Using limestone to reduce set retardation in high volume fly ash mixtures: improving constructability for sustainability. Transport Res Rec 2012;2290:139–46.
[11] ASTM Annual Book of ASTM Standards. Concrete and Aggregates. West Conshohocken; 2009.
[12] Kumar A, Bishnoi S, Scrivener KL. Modeling early age hydration kinetics of alite. Cem Concr Res 2012;42(7):903–18.
[13] Oey T, Kumar A, Bullard JW, Neithalath N, Sant G. The filler effect: the influence of filler content and surface area on cementitious reaction rates. J Am Ceram Soc 2013;21:1–13. http://dx.doi.org/10.1111/jace.12264.
[14] Torquato S. Random heterogeneous materials: microstructure and macroscopic properties. New York: Springer; 2002.
[15] Bentz DP. Three-dimensional computer simulation of portland cement hydration and microstructure development. J Am Ceram Soc 1997;80(1):3–21.
[16] Bentz DP, Aitcin P-C. The hidden meaning of water-to-cement ratio. Concr Int 2008;30(5):51–4.
[17] Bentz DP, Martys NS. Hydraulic radius and transport in reconstructed model 3D porous media. Transport Porous Med 1994;17(3):221–38.
[18] Sant G, Ferraris CF, Weiss J. Rheological properties of cement pastes: a discussion of structure formation and mechanical property development. Cem Concr Res 2008;38(11):1286–96.
[19] Bentz DP, Sant G, Weiss WJ. Early-age properties of cement-based materials: I. influence of cement fineness. ASCE J Mater Civil Eng 2008;20(7):502–8.
[20] Sant G, Dehadrai M, Bentz D, Lura P, Ferraris CF, Bullard J, et al. Detecting the fluid-to-solid transition in cement pastes. Concr Int 2009:43–8.
[21] Scherer GW, Zhang J, Quintanilla JA, Torquato S. Hydration and percolation at the setting point. Cem Concr Res 2012;42(5):665–72.
[22] Zheng J-J, Zhang J, Scherer GW. Prediction of the degree of hydration at initial setting time of cement paste with particle agglomeration. Cem Concr Res 2012;42(9):1280–5.
[23] Vance K, Aguayo M, Oey T, Sant G, Neithalath N. Hydration and strength development in ternary portland cement blends containing limestone and fly ash or metakaolin. Cem Concr Compos 2013;21:12. http://dx.doi.org/10.1016/j.cemconcomp.2013.03.028.
[24] Haecker CJ, Garboczi EJ, Bullard JW, Bohn RB, Sun Z, Shah SP, et al. Modeling the linear elastic properties of portland cement paste. Cem Concr Res 2005;35(10):1948–60.
[25] Velez K, Maximilien S, Damidot D, Fantozzi G, Sorrentino F. Determination by nanoindentation of elastic modulus and hardness of pure constituents of Portland cement clinker. Cem Concr Res 2001;31(4):555–61.
[26] Chen JJ, Sorelli L, Vandamme M, Ulm FJ, Chanvillard G. A coupled nanoindentation /SEM-EDS study on low water/cement ratio portland cement paste: evidence for C–S–H/Ca(OH)2 Nanocomposites. J Am Ceram Soc 2010;93(5):1484–93.
[27] Sandberg P, Roberts L. Cement-admixture interactions related to aluminate control. J ASTM Int 2005;2:1–14.
[28] Bentz DP, Peltz MA, Winpigler J. Early-age properties of cement-based materials: II. influence of water-to-cement ratio. ASCE J Mater Civil Eng 2009;21(9):512–7.
[29] Bentz DP, Irassar EF, Bucher B, Weiss WJ. Limestone fillers to conserve cement in low w/cm concretes: an analysis based on powers' model. Concr Int 2009;31(11):41–6.
[30] Jensen OM, Hansen PF. Water-entrained cement based materials I: principles and theoretical background'. Cem Concr Res 2001;31(4):647–54.
[31] Mindess S, Young JF, Darwin D. Concrete. 2nd ed. New Jersey: Prentice Hall; 2003. p. 656.
[32] Bentz DP, Duran-Herrera A, Galvez-Moreno D. Comparison of ASTM C311 strength activity index testing vs. testing based on constant volumetric proportions. J ASTM Int 2012;9(1):7.
[33] Bentz DP, Barrett T, De la Varga I, Weiss WJ. Relating compressive strength to heat release in mortars. Adv Civil Eng Mater 2012;1(1):14.
[34] Bentz DP. Blending different fineness cements to engineer the properties of cement-based materials. Mag Concr Res 2010;62(5):327–38.
[35] Bentz DP. Verification, validation, and variability of virtual standards. In: 12th international congress on the chemistry of cement. Montreal; 2007.
[36] Zelic J, Rusic D, Krstulovic R. A mathematical model for prediction of compressive strength in cement-silica fume blends. Cem Concr Res 2004;34:2319–28.
[37] Ioan M, Radu L, Mandoiu C. Software-enhanced method for rapid determination of the early heat of hydration of cement CEM II/A and B-S to predict the 28-day compressive strength. In: Proc of the 1st international proficiency testing conference. Sinaia, Romania; 2007, p. 355–362.
[38] Hobbs DW. Influence of aggregate restraint on the shrinkage of concrete. ACI J 1974:445–50.
[39] Garboczi EJ, Bentz DP. Analytical formulas for interfacial transition zone properties. Adv Cem Based Mater 1997;6(3–4):99–108.
[40] Barde A, Mazzotta G, Weiss WJ. Early-age flexural strength: the role of aggregates and their influence on maturity predictions, material science of concrete VII, American ceramic society. Wiley Publishers; 2005.
[41] Bentz DP, Coveney PV, Garboczi EJ, Kleyn MF, Stutzman PE. Cellular automaton simulations of cement hydration and microstructure development. Modelling and Simulation in Materials Science and Engineering 1994;2(4):783.